Weak Lensing for Precision Cosmology

Mohamed Shaaban

April 2019

1 Introduction

The most revolutionary discovery in cosmology since Hubble observed that the Universe is expanding is that this expansion is accelerating. A revelation that was awarded the 2011 Nobel Prize for its profound implications. [1]. An accelerating universe implies that either our understanding of gravity is flawed or that a mysterious negative pressure known as Dark Energy is driving the expansion [13]. This Dark Energy accounts for most (over 68%) of the energy density in the observable universe, however its origin and physics are presently unknown [2]. As a result, the nature of Dark Energy is considered one of the greatest mysteries of modern science [3].

One of the most powerful ways to probe Dark Energy, as well as modified theories of gravity, is a technique known as weak gravitational lensing, or weak lensing for short [6, 9]. Gravitational lensing is the phenomenon of light ray deflection by intervening mass. When the deflection is sufficiently weak, this phenomenon manifests in images of galaxies as a shearing effect due to the differential deflection of neighboring light rays [17, 6]. This shearing induces a subtle (sub 1%) change in the ellipticity of the images. Although such a change is negligible in comparison to the 30% dispersion in intrinsic galaxy ellipticities, it can be statistically measured by using the coherence of the lensing shear over the sky [17]. The reason weak lensing is considered very powerful is because it provides a direct measurement of the matter distribution in the universe as a function of redshift independent of any cosmological assumptions. Thus, allowing us to directly probe the growth of cosmic structure with time [6].

In this report I present a general overview of weak lensing in the context of cosmology. I begin by presenting the theory behind the Cosmology we would like to probe, as well as the general theoretical framework on which weak lensing operates. I then present the weak lensing measurment procedure and how cosmological data can be extracted from such measurements. Finally, I end this report by presenting some results from an active experiment and a short discussion on potentially concerning systematics.

2 Background Theory

2.1 Standard Model of Cosmology

The fundamental assumption in cosmology, known as the cosmological principle, is that we live in a homogenous (independent of position) and isotropic (independent of direction) universe [17, 15]. Solving Einstein's equations under the geometric symmetries provided by the cosmological principle and taking into account the expansion of the universe one finds that the dynamics of the universe are governed by the Friedman equation [15, 17],

$$H^2(z) = H_0^2 \left(\Omega_r (1+z)^4 + \Omega_m (1+z)^3 + \Omega_k (1+z)^2 + \Omega_\Lambda \frac{\rho_\Lambda(z)}{\rho_\Lambda(0)} \right) \quad (1)$$

were H is hubble's constant and Ω_i is the normalized energy density of radiation, matter, space-time curvature, and Dark Energy at $z = 0$. The parameter ρ_Λ is theoretically predicted to be a constant, however, this prediction is yet to be experimentally confirmed as the evolution of Dark Energy is experimentally unconstrained. There have been a variety of methods proposed to probe this evolution, those methods are summarized in [17]. In essence all the probes simplify to te same concept; one uses an observable to track a cosmological distance as a function of redshift. Due to report size constraints we will not include a discussion on distance measures in cosmology as it has already been extensively discussed in class. For a complete summary of cosmological distances see [7].

2.1.1 Matter Power Spectrum

[16]

2.2 Bending of Light

The fundamental concept on which weak lensing is built is gravity's ability to alter the path of a photon. This phenomenon is explored in full detail in [14, 8, 11]. In this subsection I present a simple overview of the theory behind the bending of light necessary to develop the weak lensing formalism. For more detailed calculations consult [14, 8, 11].

2.2.1 Newtonian Lens

It is a common misconception that the gravitational bending of light is an exclusive property of GR. However, gravity induced alterations to a photon's path are predicted by newtonian mechanics [12]. To illustrate this consider a mass M located at the origin of the cartesian plane and a corpuscle(newtonian photon) propagating along the $x = b$ line (in this context b is known as the impact parameter). Newton's second law predicts that the presence of the point mass will result in a momentum transfer between the two objects. If the corpuscle starts with momentum $(p, 0)$ then it will end up with momentum (p_x, p_y). Therefore,

the particle path is deflected by some angle $\hat{\alpha}$. The deflection angle is simply given by

$$\sin(\hat{\alpha}) = \frac{p_y}{\sqrt{p_x^2 + p_y^2}} \tag{2}$$

For very small deflections we have $p \approx p_x >> p_y$ and $\hat{\alpha} << 1$. Therefore Equation 2 simplifies to $\hat{\alpha} \approx \frac{p_y}{p_x}$. We now consider the infinitesimal deflection along the entire path of the photon with $d\hat{\alpha} = \frac{dp_y}{p_x} = \frac{1}{px} dx \frac{dp_y}{dx}$. Therefore, we can find the deflection angle by

$$\begin{aligned} \hat{\alpha}_N &= -\frac{1}{p_x} \int dx \frac{dp_y}{dx} \\ &= -\frac{1}{cp_x} \int dx \frac{dp_y}{dt} \\ &= \frac{2GM}{c^2 b} \end{aligned} \tag{3}$$

We note that the mass of the corpuscle cancels out of the deflection equation. Therefore this equation applies for massless particles i.e. photons. Therefore Equation 3 provides a newtonian description for the bending of light [12].

2.2.2 General Relativistic Bending of Light

The Einstein's field equations in the presence of a charge free static point mass is uniquely solved by the Schwarzchild metric [14]. The Schwarzchild metric is

$$ds^2 = \left(1 - \frac{r_s}{r}\right) dt^2 - \left(1 - \frac{r_s}{r}\right)^{-1} dr^2 - r^2 d\Omega^2 \tag{4}$$

where r_s is the Shcwarzchild radius of the system given by $r_s = 2\mu = 2GM/c^2$ and (t, r, Ω) are the standard parameters for 4D space-time in polar coordinates. We can analyze the path of the photon from subsubsection 2.2.1 by studying the geodesic equations of the metric and finding the conserved quantities of the system. We can then combine the conservation equations with the tangent vector norm condition for a null path to get the shape equation of the system as

$$\frac{d\phi}{dr} = \frac{1}{r^2} \left(\frac{1}{b^2} - \frac{1}{r^2} \left(1 - \frac{2\mu}{r}\right) \right)^{-1/2} \tag{5}$$

where (r, ϕ) are the photons position in 2D polar coordinates and b is the impact parameter. Rewriting this equation under the transformation of $r = 1/u$ and working pertrubatively around $u(\mu = 0) = \frac{1}{b} \sin\phi$ we get

$$u(\phi) \approx \frac{1}{b} \sin\phi + \frac{3\mu}{2b^2} \left(1 + \frac{1}{3} \cos 2\phi\right) \tag{6}$$

in the limit were $\phi << 1$ and $u \to 0$ Equation 6 simplifies to $\phi = \hat{\alpha}_N = \frac{2GM}{c^2 b}$. Geometrically the deflection is given by $\hat{\alpha} = 2\phi$ and therefore the deflection angle is

$$\hat{\alpha} = 2\hat{\alpha}_N = \frac{4GM}{c^2 b} \tag{7}$$

We conclude that general relativity predicts a factor of 2 greater deflection form a point mass than is predicted by newtonian mechanics. This relationship greatly simplifies the formalism developed for weak lensing.

2.3 Weak Lensing Formalism

Now that we have a theoretical understanding of the Cosmological parameters we would like to measure, as well as an understanding of how gravitational fields impact the trajectory of light. We are ready to develop the theoretical formalism on which all weak lensing applications are built. This formalism is based on a combination of the frameworks developed in these sources [8, 17, 9, 6, 10, 11, 5].

2.3.1 Weak thin lens

In order to develop our formalism let us consider a general lensing system as seen in Figure 1. For astronomical applications on cosmological scales the distance from the observer to the lens D_L, the distance from the lens to the source D_{LS}, and the distance from the observer to the source D_S are much greater than the thickness of the lens along the optical axis. Therefore we can treat the lens as a "thin lens", i.e. it lives on a planar slice (lensing plane) along the line of sight. We project the mass and potential of the lens onto the lensing plane by defining the projected surface density Σ and projected potential Φ as

$$\begin{aligned} \Sigma(x,y) &= \int \rho(x,y,z)dz \\ \Phi &= \int \phi dz \end{aligned} \tag{8}$$

were ρ and ϕ are the spatial mass density and the newtonian potential respectively. We can now use the results from the previous section to find the deflection angle $\hat{\alpha}$ due to the extended thin lens. The deflection is given by

$$\hat{\alpha} = \frac{2}{c^2}\nabla\Phi(x,y) \tag{9}$$

were the factor of 2 comes from Equation 7 and ∇ is the two dimensional gradient. Note that this equation is equivalent to that describing the deflection of light by an optical lens with refractive index $n = 1 - 2\phi/c^2$, hence the name lensing. Geometrically we have $\beta = \theta - \alpha$ and $\hat{\alpha} = \frac{D_{LS}}{D_S}\alpha$ from Figure 1. This leads us to the ray trace equation

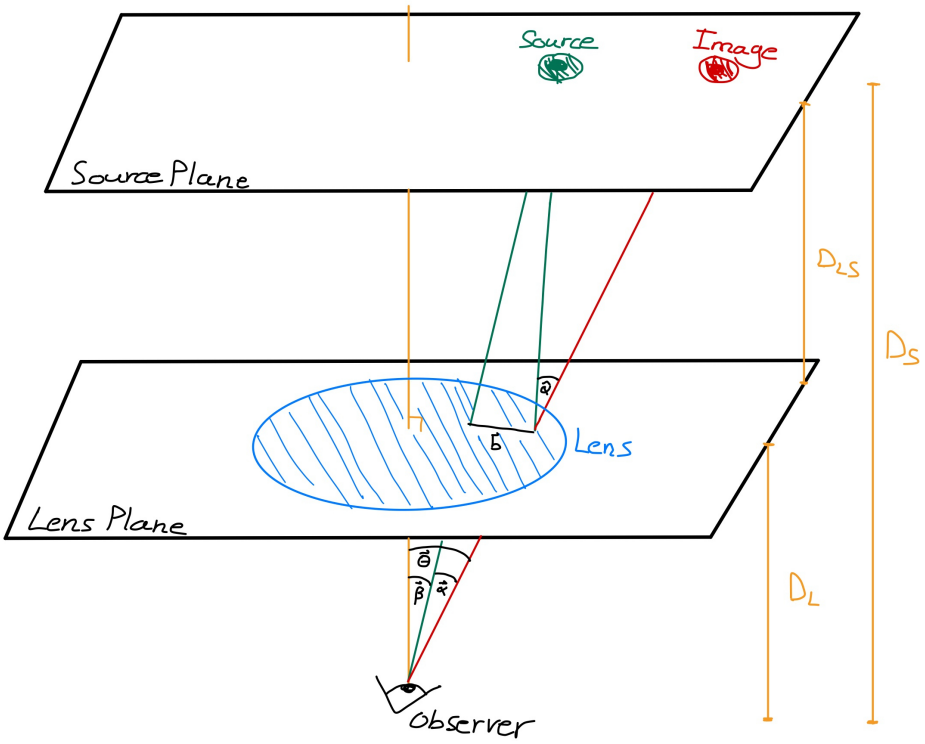

Figure 1: Sketch of a thin lens system highlighting the parameters of relevance in the weak lensing formalism. It is conventional to assume the planes are orthogonal to the z axis.

$$\beta = \theta - \frac{D_{LS}}{D_S}\hat{\alpha}(\theta) \tag{10}$$

The ray trace equation is the fundamental equation in weak lensing relating all the geometric properties of the system to one another.

2.3.2 Differential deflection of adjacent light rays

In the weak limit the actual deflections are not observable because the true position of the source is unknown. As a result, only the effects of differential deflection can be measured. Two adjacent light rays from the source pass through the lens at slightly different positions and will therefore be deflected differently. This effect results in a remapping of the observed surface brightness of the source I_s to the observed surface brightness I_{obs}. This mapping can be linearized and is therefore given by

$$I_{obs}(\vec{\theta}) \approx I_s(A\vec{\theta}) \tag{11}$$

were A is the Jacobian of the transformation. A convenient convention is to rewrite the 2D Jacobian as

$$A = \delta_{ij} - \frac{\partial^2\Phi}{\partial\theta_i\partial\theta_j} = \begin{pmatrix} 1-\kappa-\gamma_+ & -\gamma_\times \\ -\gamma_\times & 1-\kappa+\gamma_+ \end{pmatrix} \tag{12}$$

were we have defined the convergence κ shear $\gamma = \gamma_+ + i\gamma_\times$ as

$$\begin{aligned} \kappa &= \frac{1}{2}(\partial_x^2\Phi + \partial_y^2\Phi) \\ \gamma_+ &= \frac{1}{2}(\partial_x^2\Phi - \partial_y^2\Phi) \\ \gamma_\times &= \partial_x\partial_y\Phi \end{aligned} \tag{13}$$

We can now study the geometric implications of the remapping. If we consider a circular source we see that γ_+ and $\gamma_\times$ correspond to a stretching of the circle along the x/y axis and the x=y line respectively, κ corresponds to isotropic enlargement of the source's profile, and since the mapping conserves surface brightness we observe an increase of the total flux by a magnification factor

$$\mu = \frac{1}{\det A} = \frac{1}{(1-\kappa)^2 - \gamma_+^2 - \gamma_\times^2} \tag{14}$$

these geometric effects are illustrated in Figure 2. To be more specific a circular source is mapped to an ellipse with major axis $a = (1-\kappa-|\gamma|)^{-1}$ and minor axis $b = (1-\kappa+|\gamma|)^{-1}$ [10]. If we define the reduced shear as $g = \gamma/(1-\kappa)$ then an ellipse with ellipticity ϵ_{orig} is mapped to an ellipse with ellipticity ϵ_{obs} given by

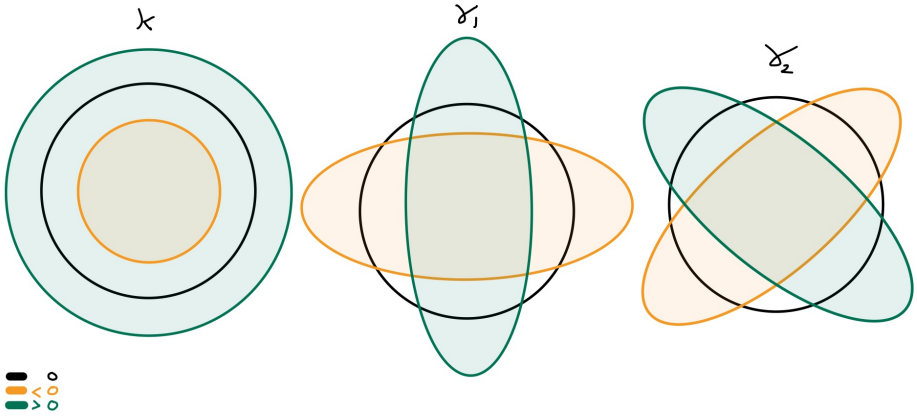

Figure 2: The effects of the convergence κ and the shear γ on a circular image of a galaxy. The black line represents the nominal image, orange represents positive parameter values, and green represents negative parameter values.

$$\epsilon_{obs} = \frac{\epsilon_{orig} + g}{1 + g^* \epsilon_{orig}} \approx \epsilon_{orig} + \gamma \tag{15}$$

the approximate relationship is a result of the weak limit ($\kappa << 1$). Equation 15 and Equation 13 demonstrate that by measuring the apparent shapes of lensed objects we are measuring information about the lensing potential and hence the matter overdensity [9, 5, 6]. Equation 15 indicates that a population of intrinsically round sources ($\epsilon_{orig} = 0$) would be ideal, but unfortunately real galaxies have an average intrinsic ellipticity of 0.25 per component [5]. Instead the lensing signal is inferred by averaging over an ensemble of sources, under the assumption that the unlensed orientations are random [9, 5]. In the next section we talk about how such measurements are made.

3 Measuring Shear (Images to Catalogs)

The weak lensing analysis process can be conceptually split into two parts; 1) converting images to catalogs of galaxy shapes and 2) extracting scientific results from shape catalogs. In this section we present a sample image to catalog pipeline. An overview of a weaklensing analysis pipeline is presented in Figure 3.

3.0.1 Object Detection

The first step in weak lensing analysis is to detect the objects that will be analyzed. In the case of cosmological data the objects of interest are faint distant galaxies. Traditional methods for galaxy detection simply involve the detection of peaks above some detection threshold in a long exposure image.

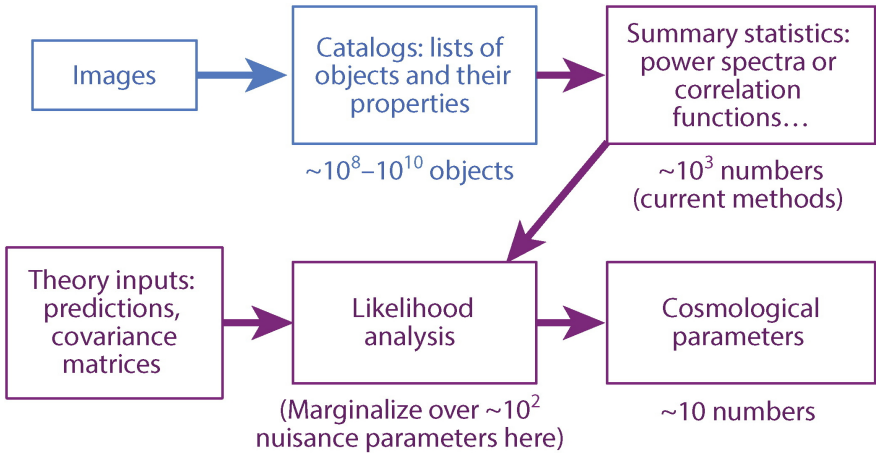

Figure 3: A generic outline of weak lensing pipeline analysis as presented in [9].

However due to the subtlety of the weak lensing signal the process is more involved. First we must confidently distinguish stars from galaxies, this is a fairly straight forward process that is usually done with photometric data. The next step is to detect galaxies that have blended together in the imaging process, i.e. detections with a double peak feature. Such blended images account for upto 10% of detections and therefore need to be either deblended or discarded from the data set [9, 17]. Finally, based on the systematics of the detector some selection criteria is introduced that will filter out problematic images.

Alternatively, another way galaxies are detected in images is by a likelihood analysis comparing imaged brightness profiles I to theoretical brightness profiles predicted by galactic theories.

3.0.2 Shape Extraction

After the galaxies are detected their shapes need to be measured. The accurate measurement of galaxy shape from an image is a rich and complex topic, we will state some results from [10, 17] without derivation. Galaxy shapes can be quantified by computing the second moments of the galaxy images

$$Q_{ij} = \frac{\int d^2x I(\vec{x}) W(\vec{x}) x_i x_j}{\int d^2x I(\vec{x}) W(\vec{x})} \tag{16}$$

were I is the brightness profile defined in Equation 11 and W is a weighting function introduced to effectively limit the domain of the integral. The exact relationship between the the second moments and ellipticity is convention dependant, in this section we will use the same definitions as [9, 5]. The size R and complex ellipticity ϵ are given by

$$R^2 = Q_{11} + Q_{22} \tag{17}$$

$$\epsilon = \frac{Q_{11} - Q_{22} + 2iQ_{12}}{Q_{11} + Q_{22}} \tag{18}$$

All ellipticity definitions have a well-defined response to a lensing shear and, hence, recover the same science after averaging across ensembles of galaxies. Equation 15 tells us that averaging over a randomly oriented galaxies gives us the mean shear ($\langle\epsilon\rangle = \langle\epsilon_{orig}\rangle + \langle\gamma\rangle = \langle\gamma\rangle$) and therefore an accurate measurement of ϵ suffices for statistical analysis.

Note that if the alternative object detection method is used, i.e. model fitting, then the ellipticity can be simply read off the best fit model without the need for computing second moments.

3.0.3 Point Spread Function

The point spread function (PSF) describes the response of an imaging system to a point source or point object. In practice the surface brightness profile of an object in an image is not the I_{obs} from Equation 11 but is convoloved with some unknown function $PSF(\vec{x})$. Therefore, in order to detect weak lensing signal we must understand and reconstruct our PSF in order to deconvolve it from the image. Deconvolving the PSF is the most important and most difficult step of any weak lensing analysis [5, 9]. The PSF has a width which leads to rounder images and typically is anisotropic, which leads to a preferred orientation. The bias is grouped into two kinds: a multiplicative bias m that scales the shear, and an additive bias c that reflects preferred orientations that are introduced. The observed shear and true shear are thus related by

$$\gamma_{obs} = (1 + m)\gamma + c \tag{19}$$

In order to take this effect the PSF must be accurately estimated and deconvolved from the results. This is done by observing a large field of stars and recording the optical systems response to a star as a function of position. The function is then estimated by interpolating between star positions.

4 Catalogs to Science

4.1 Cosmic Shear

4.2 Cosmic Tomography

For current and future surveys, one goal is to use the redshifts of the background galaxies (often approximated using photometric redshifts) to divide the survey into multiple redshift bins. The low-redshift bins will only be lensed by structures very near to us, while the high-redshift bins will be lensed by structures over a wide range of redshift. This technique, dubbed "cosmic tomography",

makes it possible to map out the 3D distribution of mass. Because the third dimension involves not only distance but cosmic time, tomographic weak lensing is sensitive not only to the matter power spectrum today, but also to its evolution over the history of the universe, and the expansion history of the universe during that time. This is a much more valuable cosmological probe, and many proposed experiments to measure the properties of dark energy and dark matter have focused on weak lensing, such as the Dark Energy Survey, Pan-STARRS, and Large Synoptic Survey Telescope. [12] [9] [6]

5 Weak Lensing Results

[4]

6 Problematic Systematics

[10]

1. PSF / detector effects
2. Blending
3. Selection Bias
4. Alignment

References

[1] The nobel prize in physics 2011 - advanced information. nobelprize.org., 2014.

[2] P. A. R. Ade et al. Planck 2013 results. I. Overview of products and scientific results. *Astron. Astrophys.*, 571:A1, 2014.

[3] K. Bandura, G. E. Addison, M. Amiri, J. R. Bond, D. Campbell-Wilson, L. Connor, J.-F. Cliche, G. Davis, M. Deng, N. Denman, M. Dobbs, M. Fandino, K. Gibbs, A. Gilbert, M. Halpern, D. Hanna, A. D. Hincks, G. Hinshaw, C. Höfer, P. Klages, T. L. Landecker, K. Masui, J. Mena Parra, L. B. Newburgh, U.-l. Pen, J. B. Peterson, A. Recnik, J. R. Shaw, K. Sigurdson, M. Sitwell, G. Smecher, R. Smegal, K. Vanderlinde, and D. Wiebe. Canadian Hydrogen Intensity Mapping Experiment (CHIME) pathfinder. In *Ground-based and Airborne Telescopes V*, volume 9145, page 914522, July 2014.

[4] Chiaki Hikage, Masamune Oguri, Takashi Hamana, Surhud More, Rachel Mandelbaum, Masahiro Takada, Fabian Köhlinger, Hironao Miyatake, Atsushi J. Nishizawa, Hiroaki Aihara, Robert Armstrong, James Bosch, Jean

Coupon, Anne Ducout, Paul Ho, Bau-Ching Hsieh, Yutaka Komiyama, François Lanusse, Alexie Leauthaud, Robert H. Lupton, Elinor Medezinski, Sogo Mineo, Shoken Miyama, Satoshi Miyazaki, Ryoma Murata, Hitoshi Murayama, Masato Shirasaki, Cristóbal Sifón, Melanie Simet, Joshua Speagle, David N. Spergel, Michael A. Strauss, Naoshi Sugiyama, Masayuki Tanaka, Yousuke Utsumi, Shiang-Yu Wang, and Yoshihiko Yamada. Cosmology from cosmic shear power spectra with Subaru Hyper Suprime-Cam first-year data. *Publications of the Astronomical Society of Japan*, page 22, Mar 2019.

[5] H. Hoekstra. Weak gravitational lensing. *Proc. Int. Sch. Phys. Fermi*, 186:59–100, 2014.

[6] H. Hoekstra and B. Jain. Weak Gravitational Lensing and Its Cosmological Applications. *Annual Review of Nuclear and Particle Science*, 58:99–123, November 2008.

[7] David W. Hogg. Distance measures in cosmology. 1999.

[8] Konrad Kuijken. The Basics of Lensing. *arXiv e-prints*, pages astro–ph/0304438, Apr 2003.

[9] Rachel Mandelbaum. Weak Lensing for Precision Cosmology. *Annual Review of Astronomy and Astrophysics*, 56:393–433, Sep 2018.

[10] Richard Massey, Henk Hoekstra, Thomas Kitching, Jason Rhodes, Mark Cropper, Jérôme Amiaux, David Harvey, Yannick Mellier, Massimo Meneghetti, Lance Miller, Stéphane Paulin-Henriksson, Sand rine Pires, Roberto Scaramella, and Tim Schrabback. Origins of weak lensing systematics, and requirements on future instrumentation (or knowledge of instrumentation). *mnras*, 429:661–678, Feb 2013.

[11] Yannick Mellier. Probing the universe with weak lensing. *Ann. Rev. Astron. Astrophys.*, 37:127–189, 1999.

[12] G. Meylan, P. Jetzer, P. North, P. Schneider, C. S. Kochanek, and J. Wambsganss, editors. *Gravitational Lensing: Strong, Weak and Micro*, 2006.

[13] P. J. E. Peebles and Bharat Ratra. The Cosmological constant and dark energy. *Rev. Mod. Phys.*, 75:559–606, 2003.

[14] A.W. Peet. General Relativity Notes . page https://ap.io/483f/files/gr1.pdf, 2018.

[15] B. Ryden. *Introduction to Cosmology*. Cambridge University Press, 2016.

[16] P. Schneider. *Extragalactic Astronomy and Cosmology*. 2006.

[17] David H. Weinberg, Michael J. Mortonson, Daniel J. Eisenstein, Christopher Hirata, Adam G. Riess, and Eduardo Rozo. Observational probes of cosmic acceleration. *physrep*, 530:87–255, Sep 2013.